



## A two-equation k- $\omega$ turbulence model simulation to narrow trench on flat plate

Antar M.M. Abdala, Qun Zheng, Fifi N.M. Elwekeel

College of Power and Energy Engineering, Harbin Engineering University, Harbin 150001, China.

### Abstract

In the present work, computational simulations was made using ANSYS CFX to predict the improvements in film cooling performance with narrow trench. Two turbulence models k- $\omega$  and k- $\epsilon$  were used. Blowing ratios in the range (0.5:1.8) were investigated. The results compared with experiments at different blowing ratios. Comparison of results with the k- $\epsilon$  model indicates that the k- $\omega$  model predicts circulations inside trench equally well at all blowing ratios. Over the surface, at low blowing ratios k- $\omega$  and k- $\epsilon$  models in case lateral spreading are under predicted but k- $\omega$  model catches experimental data well. At high blowing ratios, all turbulence models were under predicted. Simulations show that k- $\omega$  work well near the wall. Simulations show high jet penetration in cross flow for k- $\omega$  model than k- $\epsilon$  model. The CFD simulations were also used to gain a better understanding of the mechanisms responsible for improved film cooling performance

*Copyright © 2013 International Energy and Environment Foundation - All rights reserved.*

**Keywords:** Gas turbine; Narrow trench; Film cooling; Adiabatic effectiveness; Jet interaction phenomena.

### 1. Introduction

Gas turbine blades need to be effectively cooled to increase component life and reduce maintenance costs. Typically, cooling a turbine blade involves long turbulated serpentine internal passages with ribs, impingement holes, and pin fins for heat transfer enhancement along with film cooling through discrete holes to protect the blades from direct contact with hot gases. With increasing turbine inlet temperatures, modern hot gas path components may be coated with thin layers of thermal barrier coatings (TBC) made of ceramic material, such as Ytria with stabilized Zirconia. The coatings are thin and on the order of film hole sizes typically 0.5–2 mm. typically, film holes are drilled on the surface before the TBC layer is applied. The hole area may be masked, then the TBC layer is sprayed, and then the mask will be removed revealing the holes embedded in 2D trenches Lu et al [1]. Gas turbine efficiency can be significantly increased by cooling technologies. Shaped holes have proven to provide the highest adiabatic effectiveness among film cooling configurations but are expensive to manufacture. Certain configurations of cylindrical holes embedded in transverse trenches have been shown to perform similarly to shaped holes, and trenches would be cheaper to manufacture than shaped holes. Trench performance is highly dependent on the configuration, so investigating variations in depth, width, and shape is important to maximize trench effectiveness. Several studies have investigated various trench configurations.

Bunker [2] studied film holes embedded in trenches. The study presented centerline adiabatic effectiveness values for trench geometries varying in width and depth. Adiabatic effectiveness increased until a blowing ratio of  $M = 4$ , indicating that the jets remained attached to the surface at much higher blowing ratios than for simple case. The narrower trench performed slightly better than the wider trench. A trench with depth  $S/D = 0.43$  was also tested and provided the highest adiabatic effectiveness.

Waye and Bogard [3] studied the presence of trenched holes on the suction side of a vane. The narrow trench configuration provided the best adiabatic effectiveness performance. In fact, the increasing adiabatic effectiveness levels with increasing blowing ratio indicated the trench suppressed coolant jet separation.

Lu et al [4] built on the work of Bunker [2] using a transient infrared thermography technique that obtained spatial heat transfer coefficients and the adiabatic effectiveness measurements. They studied the effect of trench width and altered the exit edge of the slot. Their results showed that the film cooling holes provide higher film effectiveness when embedded in a trench. However, in some geometries, when the trench began at the upstream edge of the hole, the film effectiveness diminished.

Harrison and Bogard [5] studied film holes embedded in narrow and wide transverse trenches. Two trench widths of  $W/D = 4$  and  $W/D = 2$  were tested at a depth of  $S/D = 0.5$ . Simulations correctly predicted that the narrow trench outperformed the baseline row of cylindrical holes and the wide trench at all blowing ratios.

Jia et al [6] investigated film holes with compound angles embedded in trenches. Both  $45^\circ$  and  $90^\circ$  compound angles can further enhance the film cooling effectiveness over the axial ejection, this is mainly due to the lateral momentum component of the ejection. A lateral passage vortex is formed inside the trench which strengthens the lateral spreading of the jets. The  $45^\circ$  compound angle gives a higher film cooling effectiveness overall.

Zuniga and Kapat [7] studied effect of increasing pitch-to-diameter ratio on the film cooling effectiveness of shaped and cylindrical holes embedded in trenches. It is a known fact that increasing the pitch between holes, while maintaining all other conditions constant, decreases the average film effectiveness, however trenching has been shown to significantly increase film coverage this study.

Renze et al. [8], investigated holes embedded in a shallow cavity using large-eddy simulation (LES). Harrison and Bogard [5] used  $k-\varepsilon$  turbulence model depending on the literatures survey outcomes of simple hole although that their studies were holes embedded in trenches. Trenches studies are complicated than axial hole because of the mixing between hot and cooled fluids inside the trench is a highly unsteady process generating complex vortical structures. These conditions have effects on mechanisms of the momentum and heat exchange between the jet and the cross flow. The  $k-\omega$  model has the advantage near the walls to predict the turbulence length scale accurately in the presence of adverse pressure gradient. The  $k-\omega$  model does not involve the complex non-linear damping functions required for the  $k-\varepsilon$  model and is therefore more accurate and more robust.

As noted above,  $k-\omega$  turbulence model not available in studying narrow trench. So, in this study narrow trench was investigated by using  $k-\varepsilon$  and  $k-\omega$  turbulence models which all available in ANSYS CFX code. Several computational studies have compared adiabatic effectiveness simulations to experiments.

## 2. Computation setup

An outline of the geometry for the narrow trench is shown in Figure 1. Dimensions of computational domain are illustrated in Figure 2. Accuracy of solutions is strongly dependent upon the quality of the grid system in minimizing grid-induced errors and in resolving the relevant flow physics. In this study, a grid sensitivity study was carried out to determine the appropriate grid. Figure 3 illustrates this study for three grids – the baseline grid with 1.6 million cells, a finer grid with 2.9 million cells (adaptation 1), and a still finer grid with 3.5 million cells (adaptation 2). For the two finer grids, the additional cells were all concentrated about the film-cooling hole and the hot gas/coolant jet interaction region, where the flow physics is most complicated. From this grid sensitivity study, the baseline grid was found to give essentially the same result for the lateral adiabatic effectiveness as those from adaptation 1 and 2 grids. The final mesh sizes of narrow trench varied from 2.9-3.2 million cells depending on blowing ratio as shown in Figure 4. Simulation conditions are presented in Table 1. The results obtained in the current study were generated using ANSYS CFX code and  $k-\varepsilon$  and  $K-\omega$  turbulence models were utilized. A very fine region of cells was created on the walls to approximate  $Y^+$  values less than unity as shown in Figure 5. The convergence criterion was set to RMS residuals of  $1 \times 10^{-5}$ .

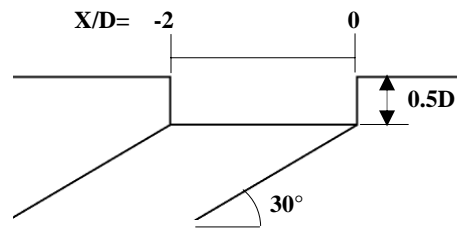


Figure 1. Test section

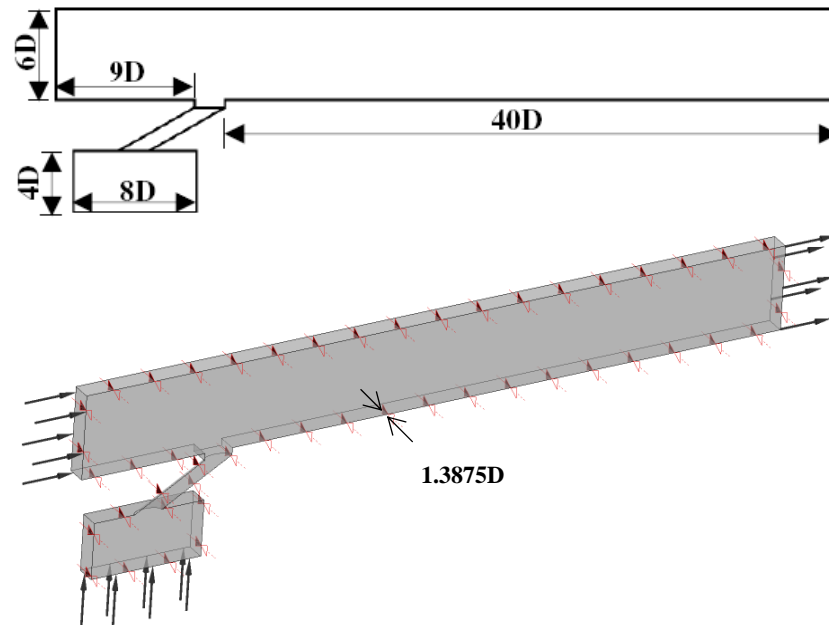


Figure 2. Dimensions of computational domain

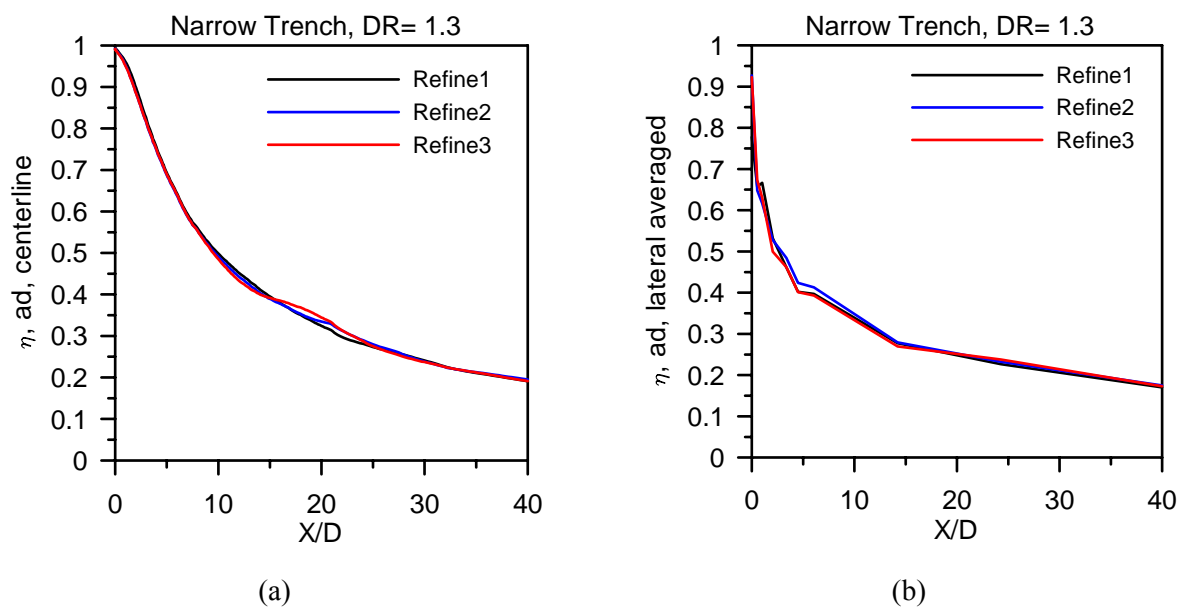


Figure 3. (a) Grid-independent study: Centerline adiabatic effectiveness for three grids; (b) Grid-independent study: Laterally averaged adiabatic effectiveness for three grids

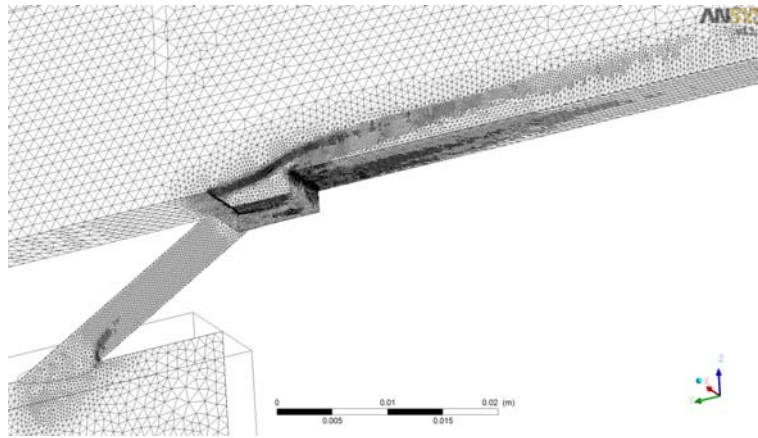


Figure 4. Computational grid for narrow trench

Table 1. Simulation parameter conditions

D	4.11 (mm)
$\alpha$	30°
L/D	5.7 (with trench) 6.7 (without trench)
P/D	2.775
S/D	0.5
DR	1.3
W/D	2D
M	0.5, 0.8, 1, 1.4 and 1.8
Mainstream conditions	
Tu	1%
$\Lambda/D$	0.42
$U_\infty$	30.82 (m/s)
T	300 (K)
Coolant conditions	
Tu	2%
$\Lambda/D$	0.56
T	230.77 (K)

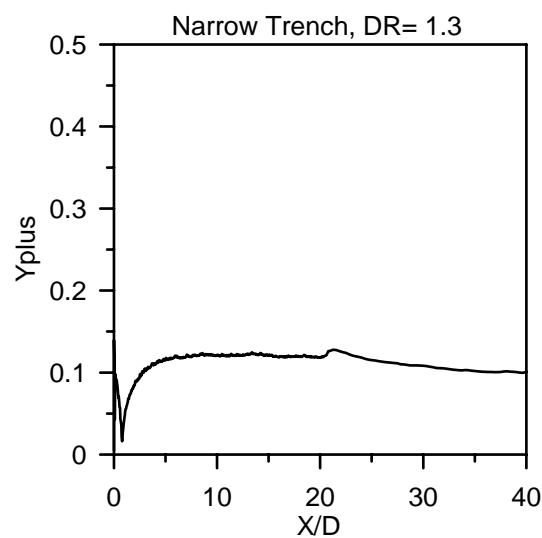


Figure 5. Y plus variations through the centerline of the plate

All flow inlets were defined as velocity inlets, while the outlet was defined as a pressure outlet. Due to symmetry, the model was cut along its half-plane and a symmetry boundary condition was applied. The plate, the hole, and the plenum walls were assigned adiabatic walls with no slip conditions. The top of the tunnel and the remaining plane were assigned walls with free slip conditions. Air was taken as a working fluid, since density variation is significant over this temperature range; the density was modeled as a function of temperature according to the following equation:

$$\rho = \frac{P}{R * T} \quad (1)$$

where,  $P$  is the reference pressure (101325 Pa),  $R$  is gas constant ( $287 \text{ J kg}^{-1} \text{ K}^{-1}$ ). The plenum inlet velocity was varied to simulate different blowing ratios. The temperature was set to 230.77 K to obtain a density ratio of  $DR = 1.3$ .

### 3. Results

In the present work, the computational domain was validated by experimental work. Contours and thermal profiles were drawn.

A comprehensive sensitivity analysis was performed against the experimental work of Sinha et al [9] for axial hole. The parameters for this sensitivity analysis, found in Table 2, were taken directly from the work of Sinha et al [9]. The simulated centre-line and lateral adiabatic film effectiveness as a function of dimensionless downstream distance are validated with the experimental work of Sinha et al [9] as shown in Figure 6 and Figure 7. The trends of adiabatic film effectiveness data follow that of Sinha et al [9].

Table 2. Sensitivity analysis properties

Property	Value
Blowing ratio	0.5 [-]
Freestream Velocity	20 [m/s]
Freestream Temperature	300 [K]
Freestream Turbulence	2 [%]
Coolant Velocity	8.33 [m/s]
Coolant Temperature	250 [K]
Coolant Turbulence	1 [%]
Hole spacing/ Diameter (P/D)	3

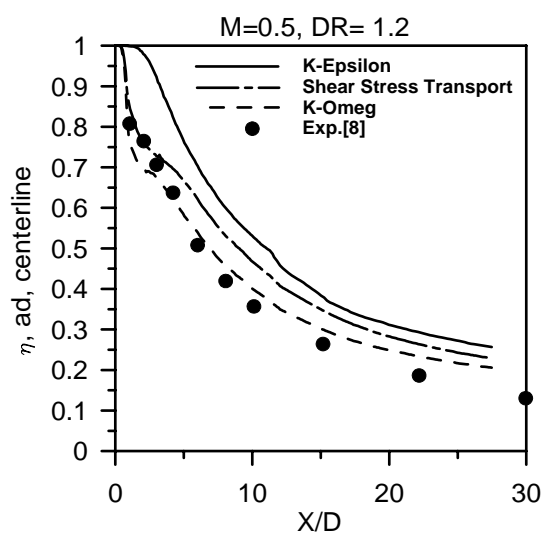


Figure 6. Validation of axial hole with experiments [8] (Centerline effectiveness)

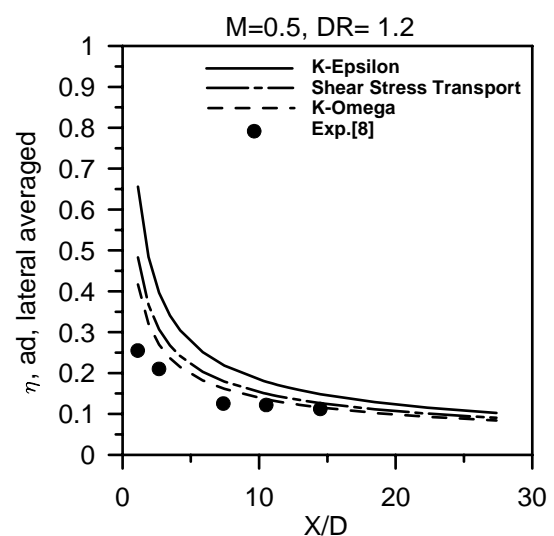


Figure 7. Validation of axial hole with experiments [8] (Lateral effectiveness)

Comparisons for narrow trench with experimental work Wayne and Bogard [3] was shown in Figures 8-11. At low blowing ratio  $M=0.5$ , the narrow trench simulation agreed very well with experimental findings.  $k-\omega$  turbulence model offers more realistic data than the others. At blowing ratio  $M=0.8$ ,  $k-\varepsilon$  turbulence model shows over predicted data than  $k-\omega$  at  $X/D > 5$ . At moderate blowing ratio  $M=1$ ,  $k-\varepsilon$  turbulence model offers close data than  $k-\omega$ . While at  $M=1.4$ , both  $k-\varepsilon$  and  $k-\omega$  turbulence models are under predicted data.

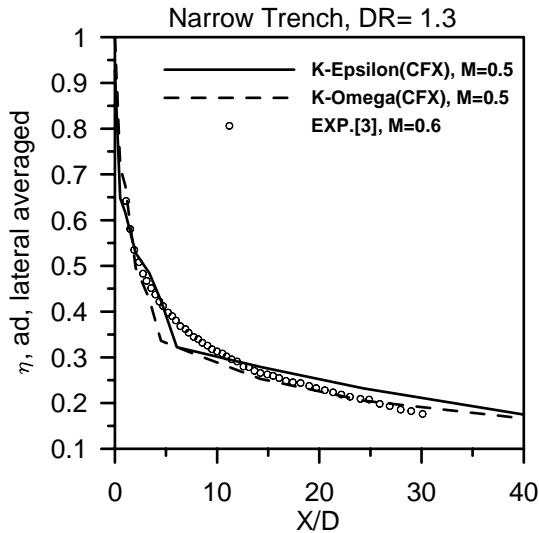


Figure 8. Validation of narrow trench with experiment [3] (Lateral effectiveness at  $M=0.5$ )

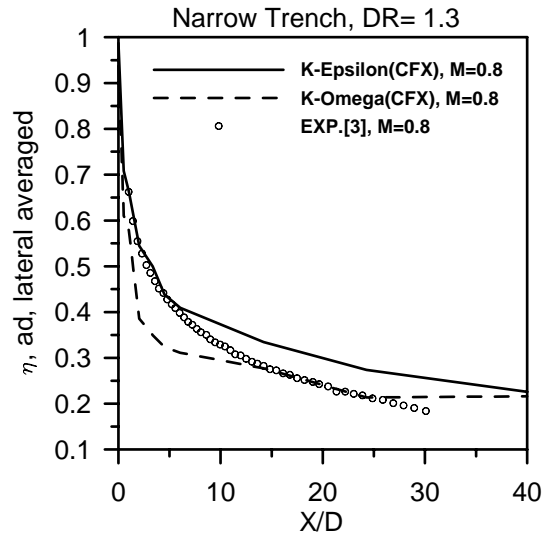


Figure 9. Validation of narrow trench with experiment [3] (Lateral effectiveness at  $M=0.8$ )

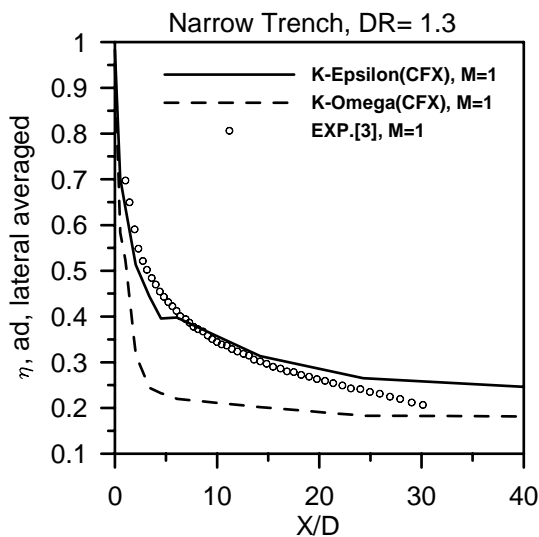


Figure 10. Validation of narrow trench with experiment [3] (Lateral effectiveness at  $M=1$ )

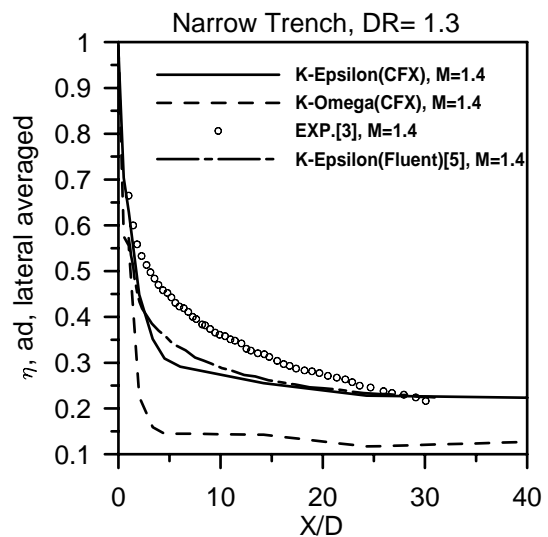
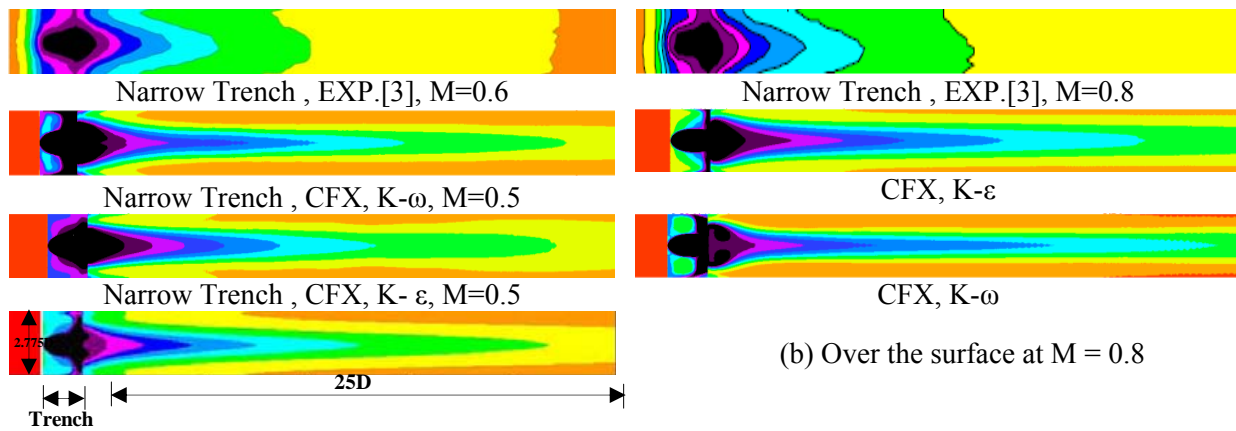


Figure 11. Validation of narrow trench with experiment [3] (Lateral effectiveness at  $M=1.4$ )

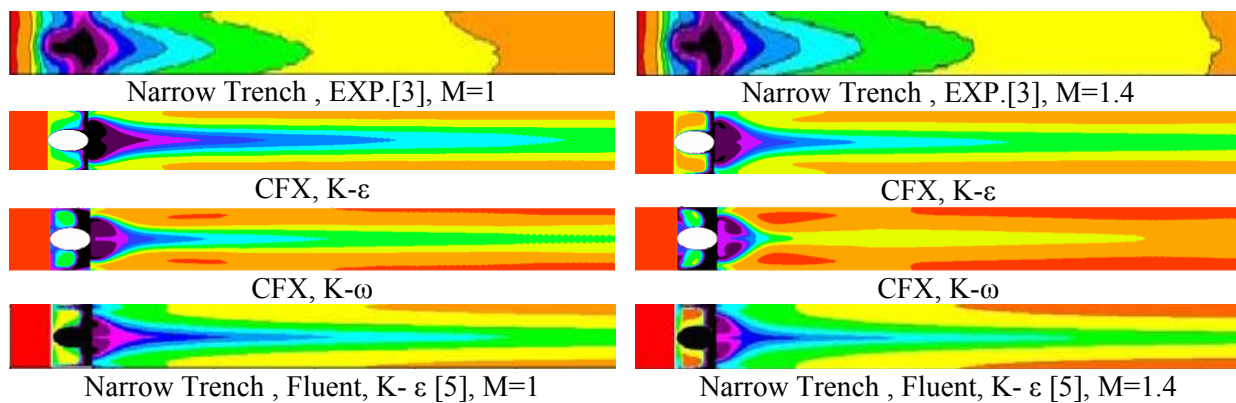
Computationally and experimentally determined contour plots of adiabatic effectiveness for the narrow trench are shown in Figure 12. The simulations clearly under-predicted lateral spreading and over-predicted centerline effectiveness for narrow trench at  $M=0.5$ ,  $0.8$  and  $1$  for each  $k-\varepsilon$  and  $k-\omega$ . At  $M=1.4$  and  $1.8$ ,  $k-\varepsilon$  simulations under-predicted lateral spreading and over-predicted centerline effectiveness, while  $k-\omega$  simulations offers under-predicted lateral and centerline effectiveness.

Figure 13 shows the experiment and simulation thermal profiles for the narrow trench at  $X/D=3$  and  $M=1$  for different turbulence models. Experiment showed that the coolant for the narrow trench case was laterally spread and attached to the surface comparing with axial hole case. Simulations produced a much rounder jet profile than measurements, which produced sharper and more triangularly shaped contours.

The general shape of the simulated contours for k-ε model is nearly close with experimental contours than k-ω model, especially at the surface and Z/D locations. All turbulence models agreed with experiment in case laterally spreading. It's cleared that k-ε model showed good attached to the surface comparing with the other turbulence model.



(a) Over the surface at M = 0.5



(c) Over the surface at M = 1.0

(d) Over the surface at M = 1.4

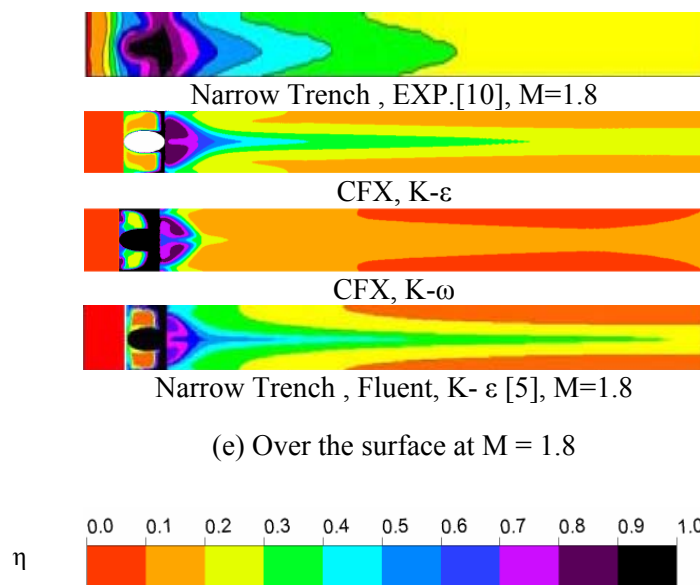


Figure 12. Surface contour plots for the narrow trench

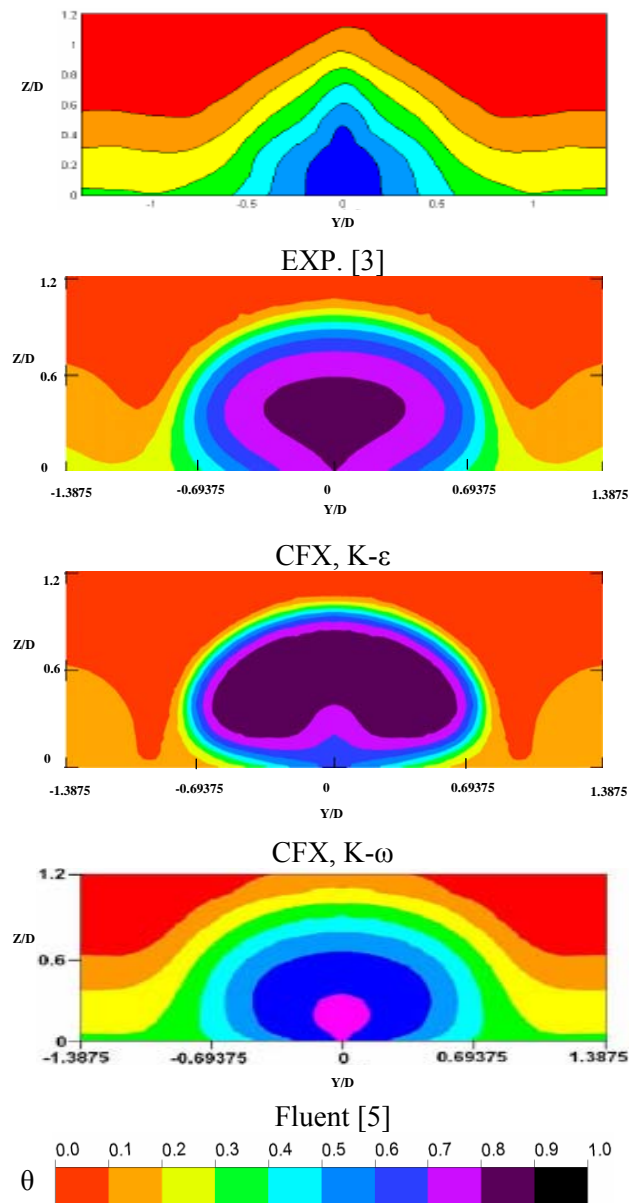


Figure 13. Contour plots for the trench over the surface at  $X/D = 3$ ,  $M = 1.0$

Computational and experimental thermal profiles locations inside the trench were examined at  $X/D = -0.5, -1, -1.5$  as shown in Figure 14. The thermal profiles at these locations are shown in Figure 15 for  $M = 1$ . By examining this simulation, it is apparent that the coolant impacted the downstream trench wall and then the coolant spread in the trench and recirculated around the hole to the back of the trench. The measurements show more coolant recirculation occurring in the trench than simulations predicted by  $k-\epsilon$  turbulence model and very good agreement by  $k-\omega$  turbulence model at all blowing ratios.

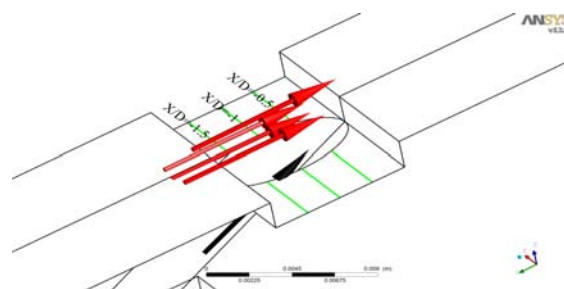


Figure 14. Definition of narrow trench plane locations



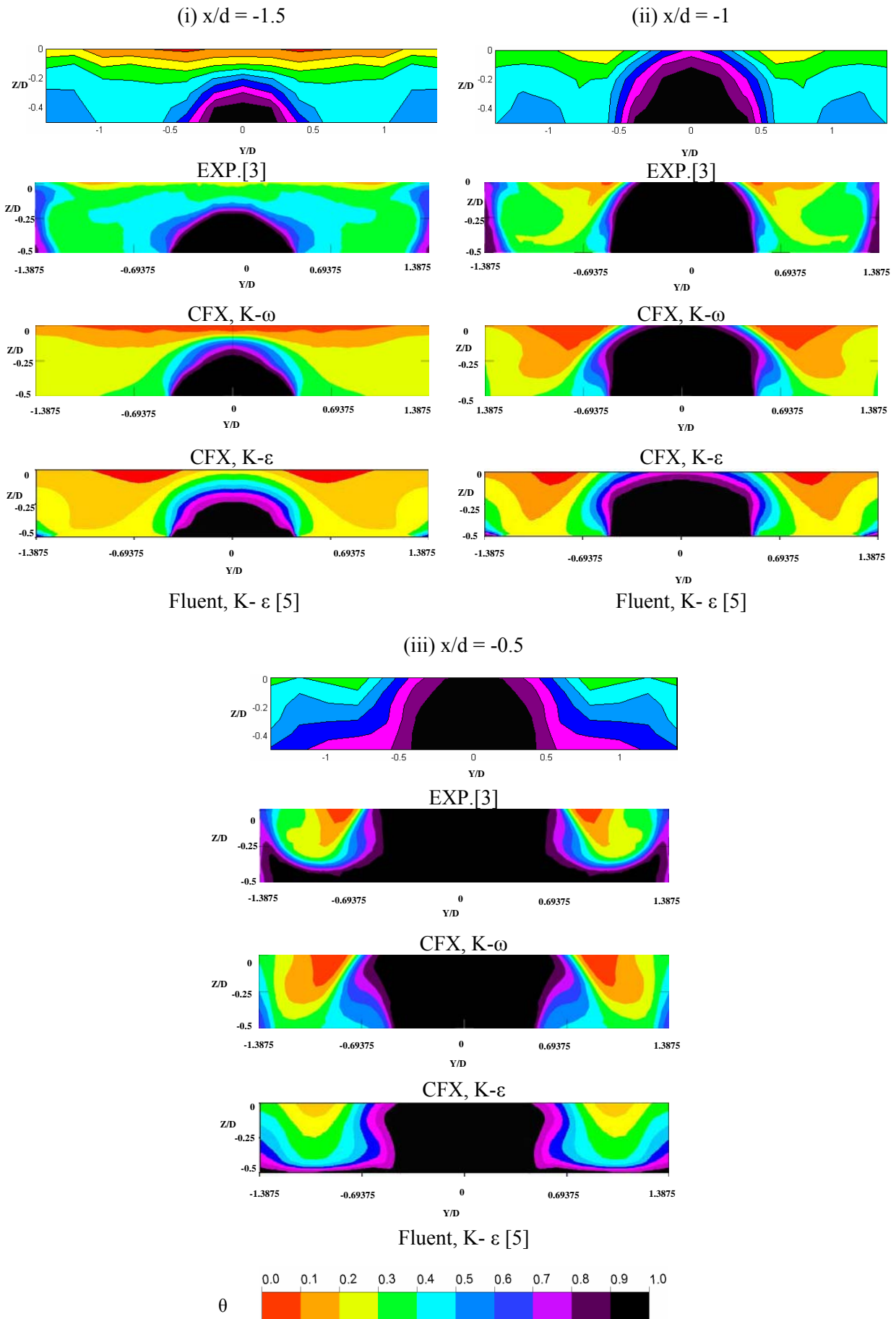


Figure 15. Computational and experimental thermal profiles inside narrow trench at  $M = 1.0$

Velocity contours for narrow trench at  $M=0.5$  and  $1.8$  for  $k-\epsilon$  and  $k-\omega$  models were shown in Figures 16, 17. It's cleared that  $k-\omega$  model calculated the velocity values larger than  $k-\epsilon$  especially inside trench. The average velocity values inside trench at shown section in case  $M=0.5$  were  $9.6$  and  $13.2$  m/s and in case  $M=1.8$  were  $39.02$  and  $42.8$  m/s for  $k-\epsilon$  and  $k-\omega$  models, respectively.

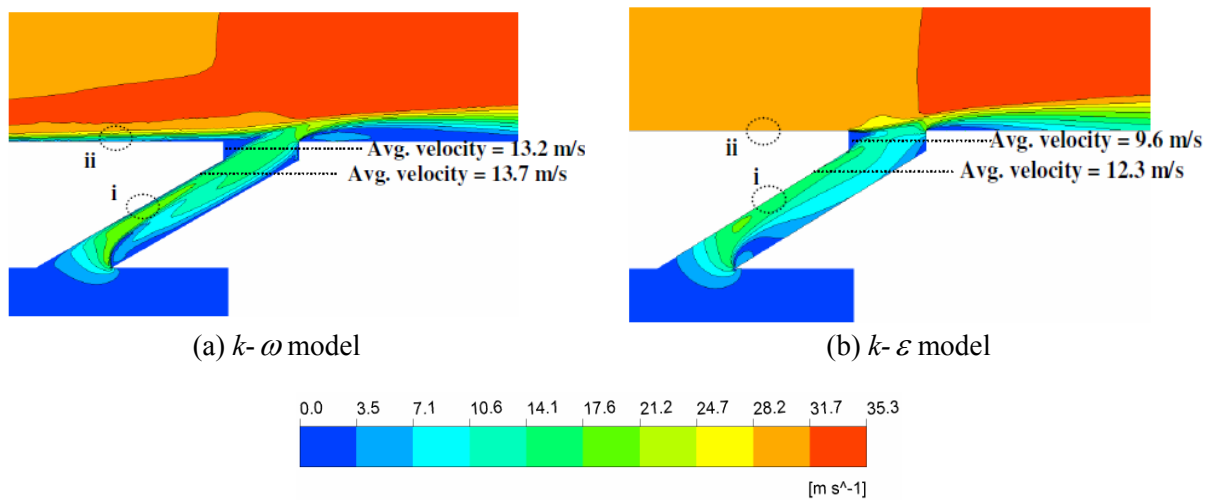


Figure 16. Velocity contours for narrow trench at  $M=0.5$

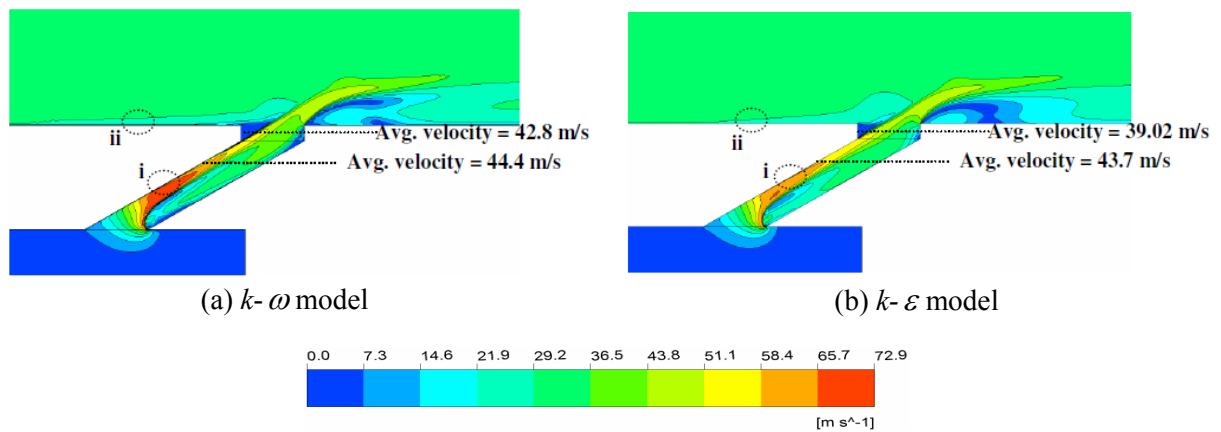


Figure 17. Velocity contours for narrow trench at  $M=1.8$

Figures 18, 19 show velocity contours near the wall at different locations for  $k-\omega$  and  $k-\epsilon$  models. It's cleared that  $k-\omega$  model catches velocity gradient near the wall well than  $k-\epsilon$  model at low and high blowing ratios. This leads to different results in effectiveness.

Figure 20 presents centerline thermal profiles for narrow trench at various blowing ratios and two turbulence models. The downstream edge of the jet interacts with the trench edge and pushes coolant toward the upstream side resulting in a larger displacement of the mainstream from the surface forming recirculation zone on the upstream edge of the trench. This recirculation zone is small or large depending on blowing ratios and turbulence models. It's cleared that  $k-\omega$  turbulence model shows high jet penetration in cross flow than  $k-\epsilon$  model. This leads to drop in centerline effectiveness at  $M > 0.8$  as shown in Figure 16.

Centerline adiabatic film effectiveness at various blow ratios with two turbulence models for narrow trench was shown in Figure 21. It's cleared that at low and high blowing ratios centerline effectiveness values for  $k-\omega$  model over and down than  $k-\epsilon$  model, respectively. At  $M=0.5$  and  $0.8$ , the effectiveness values in case  $k-\omega$  model were  $2.4\%$  and  $8.7\%$  larger than  $k-\epsilon$  model, respectively. While at high blowing ratios  $1, 1.4$  and  $1.8$ , the effectiveness values in case  $k-\omega$  model were  $21.5\%, 44.4\%$  and  $51.6\%$  less than  $k-\epsilon$  model, respectively.

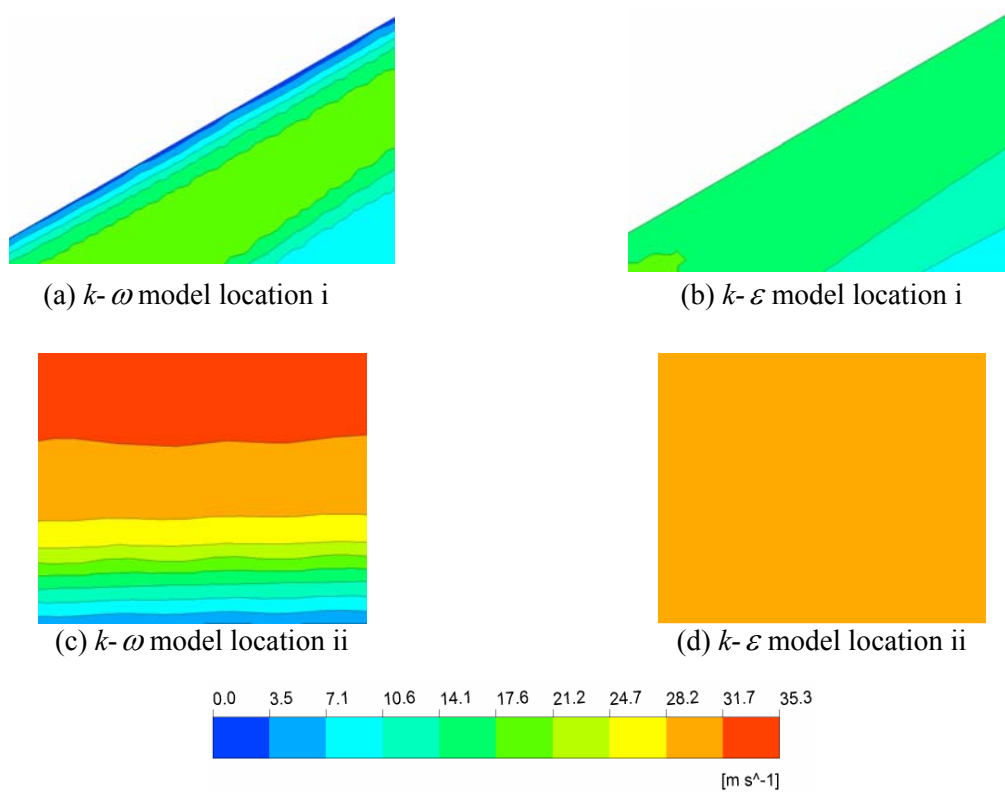


Figure 18. Velocity contours near the wall at M=0.5

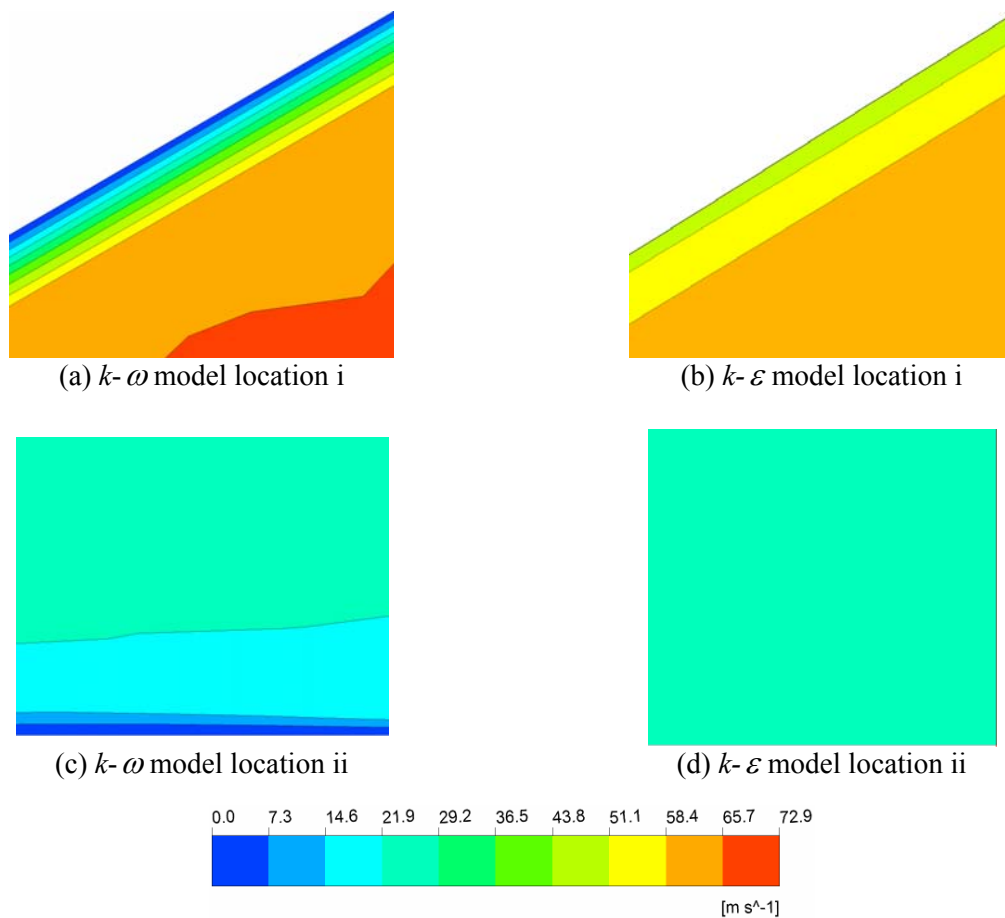


Figure 19. Velocity contours near the wall at M=1.8

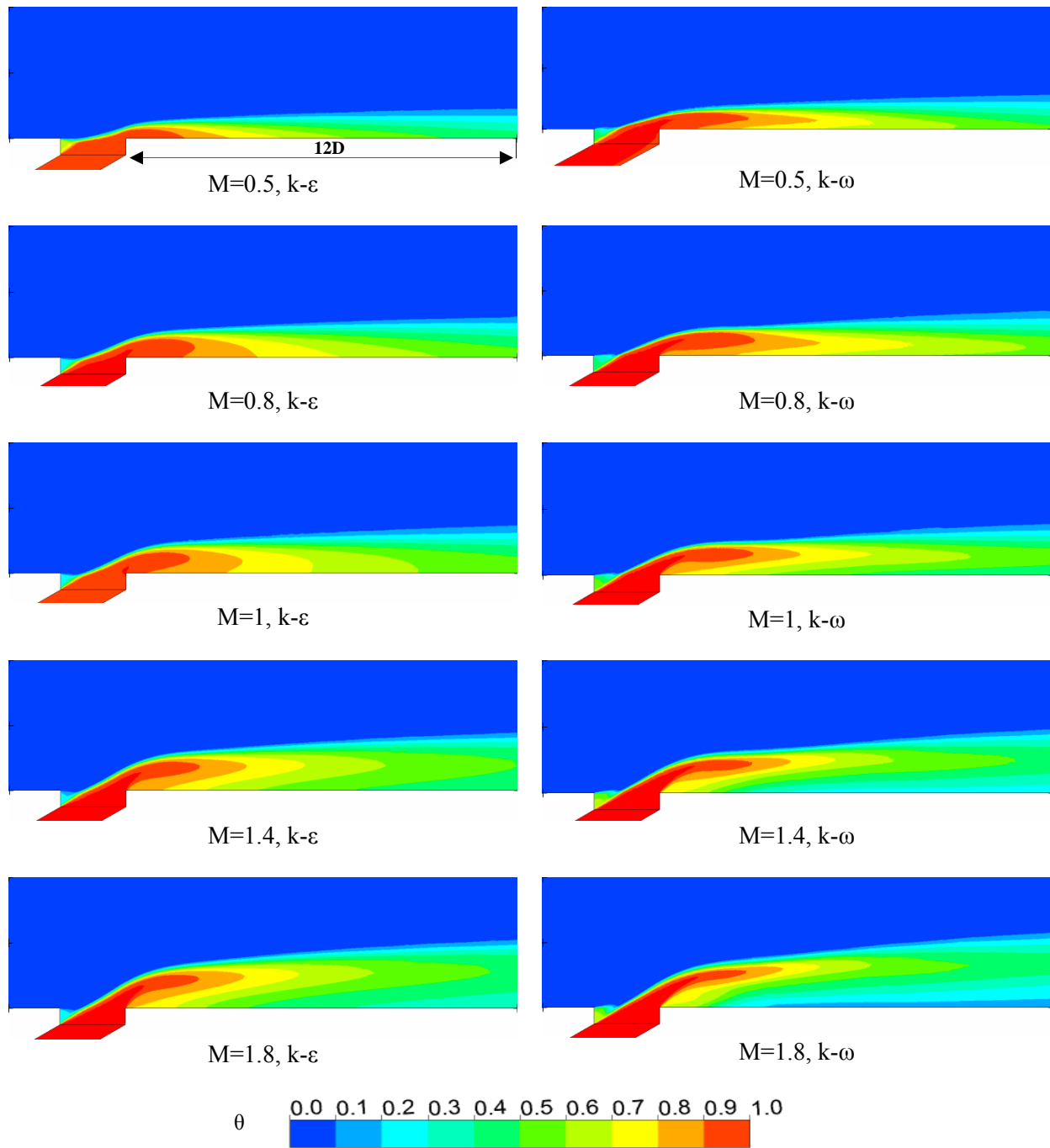


Figure 20. Centerline thermal profiles of the narrow trench

**4. Conclusions**

In this study, computational simulations were made using ANSYS CFX to predict the improvements in film cooling performance for narrow trench configuration. Two turbulence models  $k-\omega$  and  $k-\epsilon$  were used. The effects of blowing ratios on adiabatic film effectiveness are analyzed in detail. Results from the validation cases indicate that  $k-\omega$  model is better suited to adverse pressure gradient flow calculations than  $k-\epsilon$  turbulence model especially inside trench and work well near the wall.

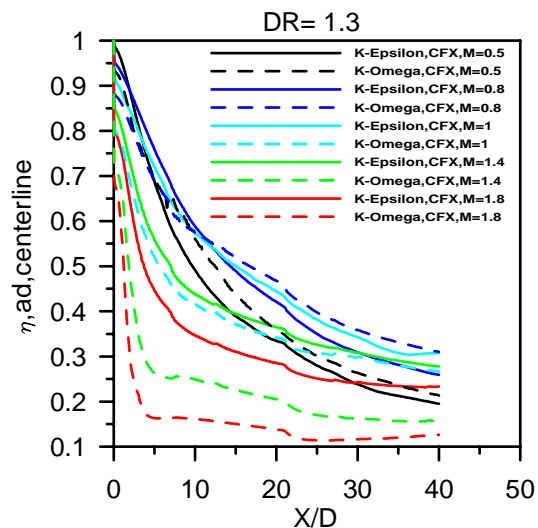


Figure 21. Centerline adiabatic film effectiveness at various blow ratios with two turbulence models for narrow trench

### Nomenclature

$D$	Hole diameter (m)
$DR$	Density ratio of coolant to mainstream, $\rho_c/\rho_\infty$ (-)
$L$	Hole length (m)
$M$	Blowing ratio of coolant to mainstream, $M = DR * U_c / U_\infty$
$P$	Hole spacing (m)
$S$	Trench depth (m)
$T$	Temperature (K)
$Tu$	Mainstream turbulence intensity (%)
$U$	Velocity (m/s)
$W$	Trench width (m)
$X$	Streamwise coordinate along model surface (m)
$Y^+$	Non-dimensional wall distance

### Greek symbols

$\lambda$	Turbulence length scale
$\alpha$	Coolant injection angle (deg.)
$\eta$	Adiabatic effectiveness, $(T_\infty - T_{aw}) / (T_\infty - T_c)$
$\theta$	Non-dimensional temperature ratio, $(T_\infty - T) / (T_\infty - T_c)$
$\rho$	Density ( $\text{kg}/\text{m}^3$ )

### Subscripts

$\infty$	Mainstream
aw	Adiabatic wall
c	Coolant

### References

- [1] Lu Y., Dhungel A., Ekkad S. V., Bunker R.S. Effect of trench width and depth on film cooling from cylindrical holes embedded in trenches. ASME Journal of Turbo machinery. 2009, 131, 1-13.
- [2] Bunker R. Film cooling effectiveness due to discrete holes within a transverse trench. ASME paper GT2002-30178. 2002.
- [3] Wayne S., Bogard D. High resolution of film cooling effectiveness measurements of axial holes embedded in a transverse trench with various trench configurations. ASME Paper GT2006-90226. 2006.
- [4] Lu Y., Nasir H., Ekkad S. V. Film cooling from a row of holes embedded in transverse slots. ASME Paper GTI2005-68598. 2005.

- [5] Harrison K. L., Bogard D. G. CFD predictions of film cooling adiabatic effectiveness for cylindrical holes embedded in narrow and wide transverse trenches. ASME Paper GT2007-28005. 2007.
- [6] Jia L., Jing R., Hongde J. Film cooling performance of the embedded holes in trenches with compound angles”, ASME Paper GT2010-22337. 2010.
- [7] Zuniga H. A., Kapat J. S. Studied effect of increasing pitch-to-diameter ratio on the film cooling effectiveness of shaped and cylindrical holes embedded in trenches. ASME Paper GT2009-60080. 2009.
- [8] Renze P., Schroder W., Meinke M. Large-eddy Simulation of film cooling flow ejected in a shallow cavity. ASME Paper, GT2008-50120. 2008.
- [9] Sinha A. K., Bogard D. G., Crawford M.E. Film cooling effectiveness downstream of a single row of holes with variable density ratio. ASME Journal of Turbomachinery. 1991, 113, 442-449.
- [10] Wayne S. Film cooling effectiveness of suction side axial holes, compound angle holes, and axial holes embedded within an overlying transverse trench. M.S. Thesis, University of Texas at Austin. 2005.



**Antar M.M. Abdala** is Ph.D. student in Power and Energy Engineering College, Harbin Engineering University, China. His major research area is Heat Transfer Applications and gas turbines blades cooling.

E-mail address: antar451@yahoo.com; Tel.: 00860 -15134554005.

**Qun Zheng** is Professor in Power and Energy Engineering College, Harbin Engineering University, China. His major research area is Performance and system analysis for ship power plant totality.

E-mail address: zhengqun@hrbeu.edu.cn

**Fifi N.M. Elwekeel** is Ph.D. student in Power and Energy Engineering College, Harbin Engineering University, China. Major research area is Heat Transfer Applications and gas turbines blades cooling.

E-mail address: ffinew2000@yahoo.com